



HAL
open science

MAVEN observations of partially developed Kelvin-Helmholtz vortices at Mars

Suranga Ruhunusiri, J. S. Halekas, J. P. Mcfadden, J. E. P. Connerney, J. R. Espley, Y. Harada, R. Livi, K. Seki, C. Mazelle, D. Brain, et al.

► **To cite this version:**

Suranga Ruhunusiri, J. S. Halekas, J. P. Mcfadden, J. E. P. Connerney, J. R. Espley, et al.. MAVEN observations of partially developed Kelvin-Helmholtz vortices at Mars. *Geophysical Research Letters*, 2016, 43, pp.4763-4773. 10.1002/2016GL068926 . insu-03670240

HAL Id: insu-03670240

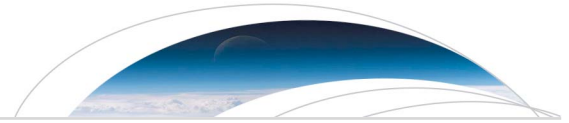
<https://insu.hal.science/insu-03670240>

Submitted on 17 May 2022

HAL is a multi-disciplinary open access archive for the deposit and dissemination of scientific research documents, whether they are published or not. The documents may come from teaching and research institutions in France or abroad, or from public or private research centers.

L'archive ouverte pluridisciplinaire **HAL**, est destinée au dépôt et à la diffusion de documents scientifiques de niveau recherche, publiés ou non, émanant des établissements d'enseignement et de recherche français ou étrangers, des laboratoires publics ou privés.

Copyright



RESEARCH LETTER

10.1002/2016GL068926

Key Points:

- Magnetosheath-ionospheric boundary oscillations observed by MAVEN are interpreted as non-fully developed Kelvin-Helmholtz vortices
- Sheath ions moving in the sunward direction is a signature of a fully developed KH vortex at Mars
- The low spatial growth rate and the small system size of Mars preclude the KH vortices from becoming fully rolled up close to Mars

Correspondence to:

S. Ruhunusiri,
suranga-ruhunusiri@uiowa.edu

Citation:

Ruhunusiri, S., et al. (2016), MAVEN observations of partially developed Kelvin-Helmholtz vortices at Mars, *Geophys. Res. Lett.*, 43, 4763–4773, doi:10.1002/2016GL068926.

Received 30 MAR 2016

Accepted 29 APR 2016

Accepted article online 6 MAY 2016

Published online 24 MAY 2016

MAVEN observations of partially developed Kelvin-Helmholtz vortices at Mars

Suranga Ruhunusiri¹, J. S. Halekas¹, J. P. McFadden², J. E. P. Connerney³, J. R. Espley³, Y. Harada², R. Livi², K. Seki⁴, C. Mazelle^{5,6}, D. Brain⁷, T. Hara², G. A. DiBraccio³, D. E. Larson², D. L. Mitchell², B. M. Jakosky⁷, and H. Hasegawa⁸

¹Department of Physics and Astronomy, University of Iowa, Iowa City, Iowa, USA, ²Space Sciences Laboratory, University of California, Berkeley, California, USA, ³NASA Goddard Space Flight Center, Greenbelt, Maryland, USA, ⁴Solar-Terrestrial Environment Laboratory, Nagoya University, Nagoya, Japan, ⁵CNRS, IRAP, Toulouse, France, ⁶University Paul Sabatier, Toulouse, France, ⁷Laboratory for Atmospheric and Space Physics, University of Colorado, Boulder, Colorado, USA, ⁸Institute of Space and Astronautical Science, JAXA, Sagami-hara, Japan

Abstract We present preliminary results and interpretations for Mars Atmospheric and Volatile Evolution (MAVEN) observations of magnetosheath-ionospheric boundary oscillations at Mars. Using centrifugal force arguments, we first predict that a signature of fully rolled up Kelvin-Helmholtz vortices at Mars is sheath ions that have a bulk motion toward the Sun. The sheath ions adjacent to a vortex should also accelerate to speeds higher than the mean sheath velocity. We also predict that while the ionospheric ions that are in the vortex accelerate antisunward, they never attain speeds exceeding that of the sheath ions, in stark contrast to KH vortices that arise at the Earth's magnetopause. We observe accelerated sheath and ionospheric ions, but we do not observe sheath ions that have a bulk motion toward the Sun. Thus, we interpret these observations as KH vortices that have not fully rolled up.

1. Introduction

While Mars has only an induced magnetosphere, it displays magnetospheric phenomena that are as diverse as in magnetized planets. Some of these phenomena include flux ropes [Vignes *et al.*, 2004; Brain *et al.*, 2010; Morgan *et al.*, 2011; Hara *et al.*, 2015], low-frequency plasma waves [Espley *et al.*, 2004; Winningham *et al.*, 2006; Gunell *et al.*, 2008; Ruhunusiri *et al.*, 2015], magnetic reconnection [Eastwood *et al.*, 2008; Halekas *et al.*, 2009; Harada *et al.*, 2015], and time-dispersed ion and electron events [Halekas *et al.*, 2015; Harada *et al.*, 2016]. While suggestive observations have been made, to date there has been no definitive identification of Kelvin-Helmholtz (KH) instability at Mars. Here we will determine whether boundary oscillations, observed by MAVEN (Mars Atmospheric and Volatile Evolution), have signatures that are consistent with our predictions for KH instability at Mars.

The Kelvin-Helmholtz instability occurs in a boundary between two fluids that flow relative to one another [Chandrasekhar, 1961]. A signature of KH instability is the formation of vortices along the boundary. The kinetic energy of the fluid motion is the source of the energy that forms and maintains these vortices. Kelvin-Helmholtz instability can arise in a variety of environments, ranging from planetary atmospheres to space plasmas.

In space plasmas, KH instability can occur due to the interaction between the solar wind and obstacles like the planetary magnetospheres [Ogilvie and Fitzenreiter, 1989; Cahill and Winckler, 1992; Chen *et al.*, 1997; Kivelson and Chen, 1995; Seon *et al.*, 1995; Fairfield *et al.*, 2000, 2003; Fujimoto *et al.*, 2003; Hasegawa *et al.*, 2004, 2006; Nykyri *et al.*, 2006; Nykyri and Otto, 2001; Chaston *et al.*, 2007; Masters *et al.*, 2010; Boardsen *et al.*, 2010; Sundberg *et al.*, 2011; Taylor *et al.*, 2012; Kavosi and Raeder, 2015], ionospheres [Terada *et al.*, 2002; Penz *et al.*, 2004; Amerstorfer *et al.*, 2007], and cometary tails [Ershkovich, 1980; Rubin *et al.*, 2012]. To date, KH vortices have been definitively identified in the magnetospheres of Mercury [Boardsen *et al.*, 2010; Sundberg *et al.*, 2011; Gershman *et al.*, 2015; Liljeblad *et al.*, 2015], Venus [Pope *et al.*, 2009], Earth [Hasegawa *et al.*, 2004, 2006; Taylor *et al.*, 2012; Kavosi and Raeder, 2015], and Saturn [Masters *et al.*, 2010, 2012; Delamere *et al.*, 2013]. This instability is important for understanding magnetospheric dynamics because it can govern the transport of energy, mass, and momentum across boundaries [Johnson *et al.*, 2014]. Kelvin-Helmholtz instability can also be a source for various ultra-low-frequency waves in the inner magnetospheres that in turn can cause

phenomenon such as energization of particles [Johnson *et al.*, 2014]. Moreover, simulations indicate that the vortical motion of KH instability generates a strongly twisted field and multiple current layers leading to reconnection [Nykyri and Otto, 2001].

Kelvin-Helmholtz instability can be an important phenomenon at unmagnetized planets, such as at Mars and Venus, because it can contribute to significant atmospheric loss [Terada *et al.*, 2002; Penz *et al.*, 2004; Möstl *et al.*, 2011]. The Automatic Space Plasma Experiment with a Rotating Analyzer instrument on board the Phobos 2 spacecraft observed strong cold ion outflows and O⁺ ion beams with energies up to several keV indicating a strong loss of plasma from the top side Martian ionosphere with an estimated rate of 10²⁵ oxygen atoms per second [Lundin *et al.*, 1990]. Motivated by this observation, Penz *et al.* [2004] estimated that the KH instability can lead to an O⁺ loss rate that is comparable to other nonthermal loss mechanisms at Mars, such as atmospheric sputtering, photochemical escape, and solar wind ion pickup. For Venus, on the other hand, Brace *et al.* [1982] have estimated that the escape ion flux in the form of ionospheric clouds alone is on the order of 10²⁶ ions per second.

A number of observations made at Mars are suggestive of the KH instability operating at its ionosphere [Acuña *et al.*, 1998; Gurnett *et al.*, 2010; Halekas *et al.*, 2011; Duru *et al.*, 2014; Ruhunusiri *et al.*, 2015; Halekas *et al.*, 2016]. For example, Mars Global Surveyor observed cold electrons above the Martian ionopause and this was interpreted as detached ionospheric clouds [Acuña *et al.*, 1998]. Similar detached ionospheric clouds were observed by the Pioneer Venus Orbiter above the Venus ionopause [Brace *et al.*, 1982], and Wolff *et al.* [1980] suggested that the formation of these detached ionospheric clouds could represent the final stage of the development of the KH instability. Gurnett *et al.* [2010], with the aid of the Mars Advanced Radar for Subsurface and Ionosphere Sounding instrument on board Mars Express, observed large amplitude electron and magnetic field turbulence in the Martian ionosphere. Kelvin-Helmholtz instability was suggested as one of the mechanisms that can be responsible for the generation of this observed turbulence. Ruhunusiri *et al.* [2015] observed that the occurrence rate of fast waves enhances near the magnetosheath-ionospheric boundary, and they suggested that the KH instability operating at this boundary can be a source of these waves.

Analytical calculations and numerical simulations suggest that the KH instability can readily develop in the Martian sheath-ionospheric boundary for certain locations depending on the solar wind flow speed. Penz *et al.* [2004], in particular, treated the solar wind flow around Mars using an MHD approximation and used the single-fluid incompressible MHD formalism for modeling the Kelvin-Helmholtz instability at the Martian sheath-ionospheric boundary. Based on this study, Penz *et al.* [2004] determined that the subsolar point is stable to the excitation of KH instability, whereas the equatorial flanks are unstable to the excitation of KH instability. The polar terminator was found to be unstable to the excitation of KH instability for medium solar wind speeds, whereas it was found to be stable for low solar wind speeds [Penz *et al.*, 2004].

Here we use the MAVEN particle and field observations to identify KH vortices at Mars. This identification was made possible by both the particle and field instrument suite on board MAVEN as well as our predictions for the signatures of KH vortices at Mars.

2. Observations

The boundary oscillations that we interpret as KH vortices were observed on 6 December 2015 as MAVEN made an orbital traversal from the magnetic pileup region/ionosphere to the magnetosheath (see Figures 1j and 1k). The MAVEN Solar Wind Ion Analyzer (SWIA) [Halekas *et al.*, 2013] detected periodic energy perturbations marked A-M with an average periodicity of 3 min, shown in Figure 1a. The perturbations are characterized by prominent reductions of energy in the sheath compared to the mean energy and broadening of energy. These perturbations can be a consequence of two scenarios: (1) the spacecraft encountering H⁺ ions in the sheath that periodically reduce their energy and (2) the spacecraft periodically encountering ionospheric regions with heavy ions that have low velocities. To distinguish between these two scenarios, we use data from the SupraThermal And Thermal Ion Composition (STATIC) [McFadden *et al.*, 2015] which has mass resolution capability. As observed in the STATIC mass spectrum, shown in Figure 1c, MAVEN indeed encountered ionospheric regions populated with heavy ions. These heavy ions are mainly O⁺ and O₂⁺. The total ion mass density increases at the times of these encounters with heavy ion populations, shown in Figure 1d. Ion pressure (see Figure 1e) also shows prominent enhancements coinciding with these heavy ion encounters in the sheath. The magnetic field, measured by the MAVEN magnetometer [Connerney *et al.*, 2015], also has significant perturbations associated with these periodic heavy-ion region encounters, shown in Figure 1b.

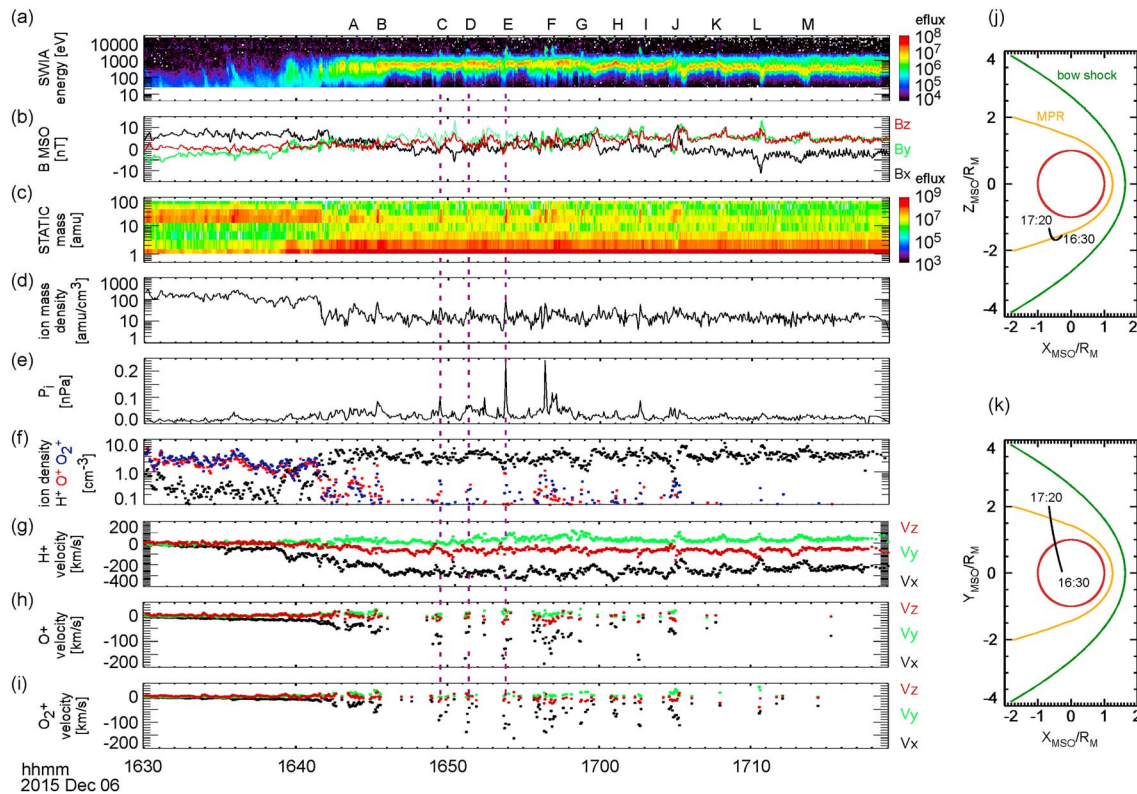


Figure 1. Boundary oscillations as observed by particle and field instruments aboard MAVEN. (a) SWIA energy spectrum displays periodic reductions in ion energy marked by A-M (b) Magnetometer observed magnetic field perturbations associated with these boundary oscillations. (c) STATIC mass spectrum shows that the boundary oscillations are characterized by periodic encounters of heavy ions. (d) Ion mass density from STATIC. (e) Ion pressure from STATIC P_i is the total pressure of individual ion species ($P_i = \sum_s P_s$ where P_s is the pressure of ion species s). (f) Ion densities for the dominant species, namely H^+ , O^+ , and O_2^+ . (g–i) Ion velocities for H^+ , O^+ , and O_2^+ , respectively, in MSO coordinates. Ion densities and velocities are only shown when the species density exceeds 0.1 cm^{-3} , because for very low densities the ion moments can be unreliable due to sensor noise and straggling. (j and k) MAVEN orbit plots in MSO coordinates. The boundary oscillations were observed when the spacecraft was in the negative MSO-z hemisphere.

To unravel the characteristics of each of the main species observed, namely, H^+ , O^+ , and O_2^+ , we plot their density and velocity in Figures 1f–1i. Both the H^+ density and H^+ X-MSO velocity component (the dominant velocity component) decrease corresponding to the boundary oscillations. The H^+ X-MSO velocity also shows periodic enhancements on either side of the times where heavy ions are encountered (see Figure 1g). As we discuss later this is in contrast to what would be expected for mass loading. The heavy-ion density and the X-MSO component of the velocity both increase (see Figures 1f, 1h, and 1i). These density and velocity data will help us to identify signatures associated with KH vortices as we describe below.

3. Interpretation

Now we will demonstrate that the observations are consistent with KH vortices that are in development or that are not fully rolled up at the sheath-ionospheric boundary at Mars.

A characteristic of rolled up vortices at Earth is magnetospheric ions traveling faster than sheath ions [Takagi et al., 2006; Hasegawa et al., 2006; Kavosi and Raeder, 2015]. This signature has been used to identify KH vortices at the Earth’s magnetopause using single-spacecraft data. The Martian sheath-ionospheric boundary is generally different from the Earth’s magnetopause. Thus, we cannot expect similar signatures for KH vortices that arise at Mars. To determine their signatures, we must consider the physics of vortex formation.

During vortex formation, centrifugal forces of the two plasma fluids participating in the rolling up motion must be equal and opposite in the vortex frame, i.e., $\rho_s V_{SKH}^2 / r^2 = \rho_l V_{IKH}^2 / r^2$. Here V is the ion flow velocity, ρ is the ion mass density, and r is the radius of the vortex structure. Subscripts S and l in the above equation denote the magnetosheath and the ionospheric regions, respectively. Now let’s consider the vortex formation at Mars’s sheath-ionospheric boundary (Figure 2). Here we consider vortex formation under ideal conditions;

KH vortex development at Mars

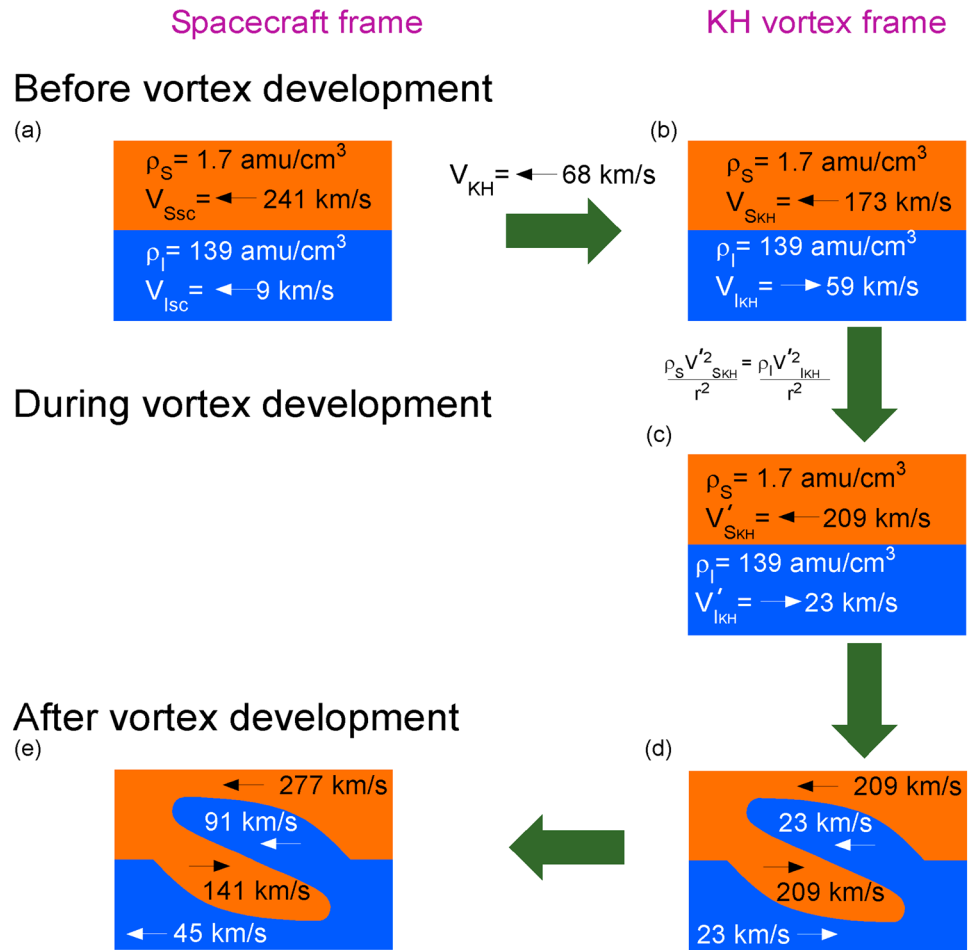


Figure 2. Physics of vortex formation in the Martian sheath-ionospheric boundary. The sheath is at the top (orange colored region) and the ionosphere is at the bottom (blue colored region). (a) Sheath and ionospheric parameters in the spacecraft frame. For magnetosheath values of the mass density and the flow velocity, we use their mean values from 17:15 to 17:25 and for the corresponding ionospheric parameters, we use their mean values from 16.30 to 16.40. (b) Sheath and ionospheric parameters in the KH vortex frame. (c) Sheath and ionospheric parameters in the KH vortex frame during the KH vortex development. (d) Sheath and ionospheric ion velocities in the KH vortex frame after vortex development. (e) Sheath and ionospheric ion velocities in the spacecraft frame after vortex development. For a fully developed vortex, the sheath ions should have a bulk velocity that is directed sunward. This occurs in the lower part of the vortex or the vortex region that is constituted by the sheath ions. The ionospheric ions are accelerated during the vortex formation; however, their velocities cannot exceed that of the sheath ions, unlike for the KH vortices at Earth.

and thus, we assume that the plasma motion is incompressible. In the spacecraft frame, shown in Figure 2(a), the sheath has a low mass density and a high flow speed, whereas the ionosphere has a very high mass density and a small flow speed (These trends can be seen in Figures 1d and 1g). To compute the velocities of ions in the sheath and ionosphere during vortex formation requires the vortex frame velocity V_{KH} . MHD simulations suggest that the KH vortex frame velocity lies between the mean velocity $((V_S + V_I)/2)$ and the center of mass velocity $(\rho_S V_S + \rho_I V_I)/(\rho_S + \rho_I)$ [Hasegawa *et al.*, 2009]. The plasma beta during this observation was comparable to one, and the MHD formalism is applicable in describing the KH vortex formation. Thus, here we assume that V_{KH} lies exactly between the mean velocity and the center of mass velocity (we assume that V_{KH} is equal to the average of the mean velocity and the center of mass velocity). In the KH vortex frame the sheath ions flow with a flow speed which is opposite to that of the ionospheric ions (see Figure 2b). Since in the KH vortex frame $\rho_S/\rho_I \approx 0.01$ and $V_I^2/V_S^2 \approx 0.1$, the ionospheric ion velocity must reduce and the magnetosheath ion velocity must increase during the vortex formation in order to achieve equal and opposite centrifugal forces

as shown in Figure 2c. Now we transform these velocities attained by the ionospheric ions and sheath ions during the vortex formation (shown in Figure 2d) back into the spacecraft frame (shown in Figure 2e). So our predictions for a fully developed vortex are as follows:

1. Sheath ions adjacent to the upper part of the vortex travel antisunward faster than their original speed.
2. Ionospheric ions that are in the upper part of the vortex (segment of the vortex that has penetrated into the sheath side) travel antisunward with a speed faster than their original speed in the ionosphere. However, their speed does not exceed that of the sheath ions.
3. Sheath ions that are in the lower part of the vortex (segment of the vortex that has penetrated into the ionospheric side) travel sunward.
4. Ionospheric ions adjacent to the lower part of the vortex travel antisunward faster than their original speed.

When the KH vortex is in its initial developing stage, it does not have a fully developed lower part or in this case a fully developed sheath region that is immersed in the ionospheric side (For example, see Figure 1a in Hasegawa *et al.* [2006]). Thus, we should not expect to observe sunward moving sheath ions as stated in prediction 3 for a vortex that is in its development stage. While ionospheric ion acceleration (signature 2) is common for mass loading, signature 1 is inconsistent with this phenomenon. Thus, signature 1 enables us to distinguish KH vortices from mass loading.

To verify whether these predictions are indeed observed, now we plot density versus velocity graphs for H^+ , O^+ , and O_2^+ using STATIC data. Such plots of density and velocity have been used for identifying faster than sheath moving magnetospheric plasma associated with KH vortices at Earth [Takagi *et al.*, 2006; Hasegawa *et al.*, 2006; Kavosi and Raeder, 2015]. Most of the H^+ ions encountered in the boundary oscillation region have antisunward velocities that are higher than their mean sheath velocity (marked by a red solid ellipse in Figure 3a). This observation is consistent with spacecraft encounters of regions adjacent to the upper regions of vortices in accordance with our prediction 1 above. This signature is also in contrast to mass loading signatures in which the H^+ ions slow down, not accelerate. We find that heavy ions in the boundary oscillation region, both O^+ and O_2^+ , move antisunward (in the negative X-MSO direction) with a significantly higher velocity than their antisunward velocity in the ionosphere (marked by red solid ellipses in Figures 3b and 3c). This observation is consistent with spacecraft encounters of upper regions of vortices consisting of heavy ionospheric ions in accordance with our prediction 2 above. While mass loading also leads to velocity increase for ionospheric heavy ions [Lundin *et al.*, 1991], this velocity increase should be much smaller than the observed velocity increase. In a mass loading boundary, the heavy ions attain a velocity of $V_i = V_s(1 - \exp(-n_s M_s / n_i M_i))$ where n_s and M_s are the density and the mass of sheath ions and n_i and M_i are the density and mass of ionospheric ions. This expression predicts an O^+ ion velocity increase by 12 km/s and O_2^+ ion velocity increase by 6 km/s in the antisunward direction. However, as can be seen in Figures 3b and 3c, the heavy ions attain much larger velocity increases.

A smaller fraction of ionospheric H^+ ions have enhanced antisunward velocities compared to their mean velocity in the ionosphere (marked by dashed ellipse in Figure 3a). This is consistent with spacecraft encounters of regions adjacent to the lower part of vortices in accordance with our prediction 4. While we do not find H^+ ions that have bulk velocities toward the Sun, we find that a smaller fraction of the H^+ ions in the boundary oscillation region have velocities significantly lower than that of the mean sheath velocity (marked by a dashed ellipse in Figure 3a). This is consistent with encounters of vortices that are in their growth phase or vortices that have not fully rolled up. Analogously, the absence of faster than sheath moving magnetospheric ions for some events at Earth has been interpreted as a signature of KH vortices that were not fully rolled up [Kavosi and Raeder, 2015].

The boundary oscillations are observed in the negative MSO-z hemisphere. Thus, if these are indeed KH vortices, the heavy ions tend to develop bulk velocities that are perpendicular to the boundary directed toward negative MSO-z direction, as depicted in Figure 3j. An examination of the MSO-z velocity and density plots for heavy ions indeed reveals this feature (see Figures 3e and 3f). Another phenomenon that arises as a consequence of the vortex development is the twisting of magnetic field in the direction of the vortex motion as shown in Figure 3k. According to Ampere's law, this twisted magnetic field topology should give rise to currents directed toward the vortex [Masters *et al.*, 2010], similar to J_A and J_B shown in Figure 3k. Currents J_A and J_B should in turn lead to cross field currents J_{C1} and J_{C2} and return currents J_{RA1} , J_{RA2} , J_{RB1} , and J_{RB2} [Masters *et al.*, 2010]. Currents J_A and J_B and the return currents should manifest in the density-velocity plots of the ions as plus and minus Y-MSO-directed ions. Inspection of the density-velocity plots for H^+ , O^+ , and O_2^+ ,

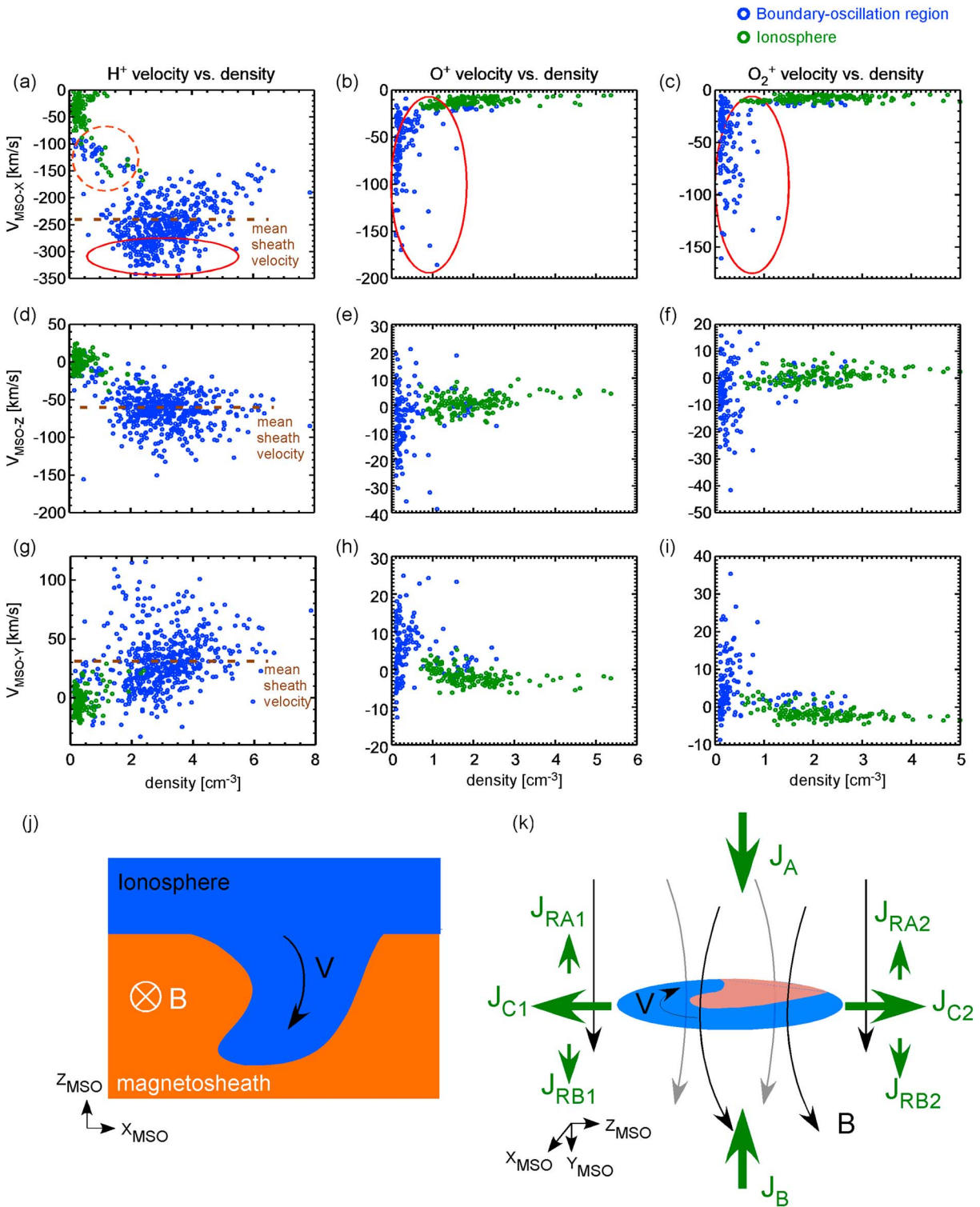


Figure 3. Density versus velocity plots for identifying signatures of KH vortices. (a–c) Density and X-MSO velocity plots for H⁺, O⁺, and O₂⁺. (d–f) Density and Z-MSO velocity plots for the three species. (g–i) Density and Y-MSO velocity plots for the three species. Ionospheric values correspond to the time interval 16:30 to 16:40, whereas the boundary oscillation region values correspond to the time interval 16:40 to 17:15. (j) Ionospheric ions tend to develop a flow toward the negative Z-MSO direction as vortices develop, and this feature is seen in Figures 3d–3f. (k) The magnetic field becomes twisted when the vortex develops and leads to vortex-directed and return currents consisting of plus and minus Y-MSO-directed ion flows as seen in Figures 3g–3i.

Figures 3g–3i, in fact reveal these plus and minus Y-MSO-directed ions. The $J \times B$ forces resulting from these currents act to resist the twisting of the magnetic field induced by the vortex motion.

Now we answer the question why these vortices are not fully rolled up. To answer this question, we need to estimate the growth rate of the KH instability at the sheath-ionospheric boundary. For this we use the growth rate (linear growth rate) expression used by Penz *et al.* [2004]: $\gamma = \left(k^2 \frac{\rho_S \rho_I (V_I - V_S)^2}{(\rho_S + \rho_I)^2} + 2k^3 \frac{(v_S + v_I) \rho_S \rho_I (V_I - V_S)}{(\rho_S + \rho_I)^2} - k^4 \frac{(v_I \rho_I - v_S \rho_S)^2}{(\rho_S + \rho_I)^2} - kg \frac{(\rho_I - \rho_S)}{(\rho_S + \rho_I)} \right)^{\frac{1}{2}}$, where g is the gravitational acceleration and $\nu = m_i V^2 / (4qB)$ is the viscous coefficient. This growth rate expression contains effects such as gravity, finite Larmor radius, and viscous effects. Using mean values of velocities and mass densities in the sheath and ionospheric regions (as used in Figure 2) and also using $g = 0.9 \text{ ms}^{-2}$, $B_S = 4.4 \text{ nT}$, $B_I = 2.1 \text{ nT}$, $m_S = m_p$, and $m_I = 26m_p$ (mean mass of ions in the ionospheric region where m_p is the mass of the proton), we find that the maximum growth rate is $8 \times 10^{-3} \text{ s}^{-1}$. The spatial growth rate corresponding to this temporal growth rate is given by $k_i = \gamma / (\frac{\partial \omega}{\partial k}) = \gamma / V_g$ where V_g is the group velocity of the disturbance. For V_g we assume the mean velocity of 68 km/s that we used as the KH vortex frame velocity, and this yields $k_i = 1.2 \times 10^{-4} \text{ km}^{-1}$. Thus, if the KH vortices have an initial amplitude of A_0 when they are made unstable, at a distance of δd along the sheath-ionospheric boundary, they should have an amplitude of $A_0 e^{(k_i \delta d)}$. Thus, if we assume that the KH instability is made unstable at the subsolar point, since they are seen at a distance of 9100 km along the sheath-ionospheric boundary, the KH vortex amplitude at the MAVEN observation point should be roughly 3 times its initial perturbation amplitude. However, as demonstrated by Penz *et al.* [2004], the subsolar point is stable to the development of KH vortices for either medium or high solar wind speeds. Thus, if we assume that the KH instability is excited between the subsolar point and the terminator, the effective distance traveled by the KH vortices is reduced and the observed amplitude at the position of the spacecraft should be lower than 3 times its initial perturbation amplitude. This means that the KH vortex amplitude increases by only few times its initial amplitude at the observation location. To become fully rolled up, the KH vortex should become nonlinear or that its amplitude should increase by a large factor. Thus, the estimated amplitude increase is insufficient to create fully rolled up vortices.

Compressibility suppresses the KH growth rate for plasma flowing at high Mach numbers [Miura and Pritchett, 1982; Miura, 1992], and this effect is not included in the growth rate expression above. The KH vortices have a positive linear growth rate with a value equal to the above growth rate when the ionospheric and the sheath flow velocities with respect to the KH vortex frame are subfast magnetosonic, i.e., $V_{IKH}/V_{FM} < 1$ and $V_{SKH}/V_{FM} < 1$ where $V_{FM} = \sqrt{V_A^2 + C_S^2}$ is the fast magnetosonic speed [Miura and Pritchett, 1982]. Here V_A is the Alfvén speed and C_S is the sound speed. When the flow velocities are superfast magnetosonic, i.e., $V_{IKH}/V_{FM} > 1$ and $V_{SKH}/V_{FM} > 1$, the KH vortices no longer have a positive linear growth rate. Instead, at these large flow speeds, nonlinear processes start to govern the growth of KH vortices and the KH vortices grow nonlinearly at a reduced growth rate [Miura, 1992]. It is not necessary for the KH vortices to have nonlinear amplitudes or that they have to be fully rolled up to have their growth governed by nonlinear processes. We find that the ionospheric and sheath flow velocities corresponding to our observation are in fact superfast magnetosonic with $V_{SKH}/V_{FM} = 3.1$ and $V_{IKH}/V_{FM} = 3.6$. Thus, when the MAVEN observes these KH vortices, they should no longer be growing at a growth rate equal to $k_i = 1.2 \times 10^{-4} \text{ km}^{-1}$ but rather at a reduced growth rate. When we take this into account, the ratio between the amplitude of the KH vortices at the location of MAVEN to their initial amplitude should become even smaller than our previous estimates. Thus, this reduction in the growth rate further aids the vortices to remain in a non-fully rolled up state. However, these vortices may form fully rolled up states farther downstream.

An interesting feature to note here is the large pressure perturbations associated with these boundary oscillations (see Figure 1e). Such large pressure perturbations are observed for fully developed KH vortices at Earth [Hasegawa, 2012]. However, since we determined that the KH vortices are not fully developed, what could be causing such large pressure perturbations? Simulations show that when the flow velocities on either side of the boundary are superfast magnetosonic, the KH vortices act as obstacles to these flows and generate shock structures [Palermo *et al.*, 2012; Miura, 1995]. As discussed above, at the MAVEN location, the ionospheric and sheath flows are superfast magnetosonic and can lead to the generation of these shock structures. The observed large pressure fluctuations are indicative of the formation of these shock structures adjacent to the non-fully developed KH vortices.

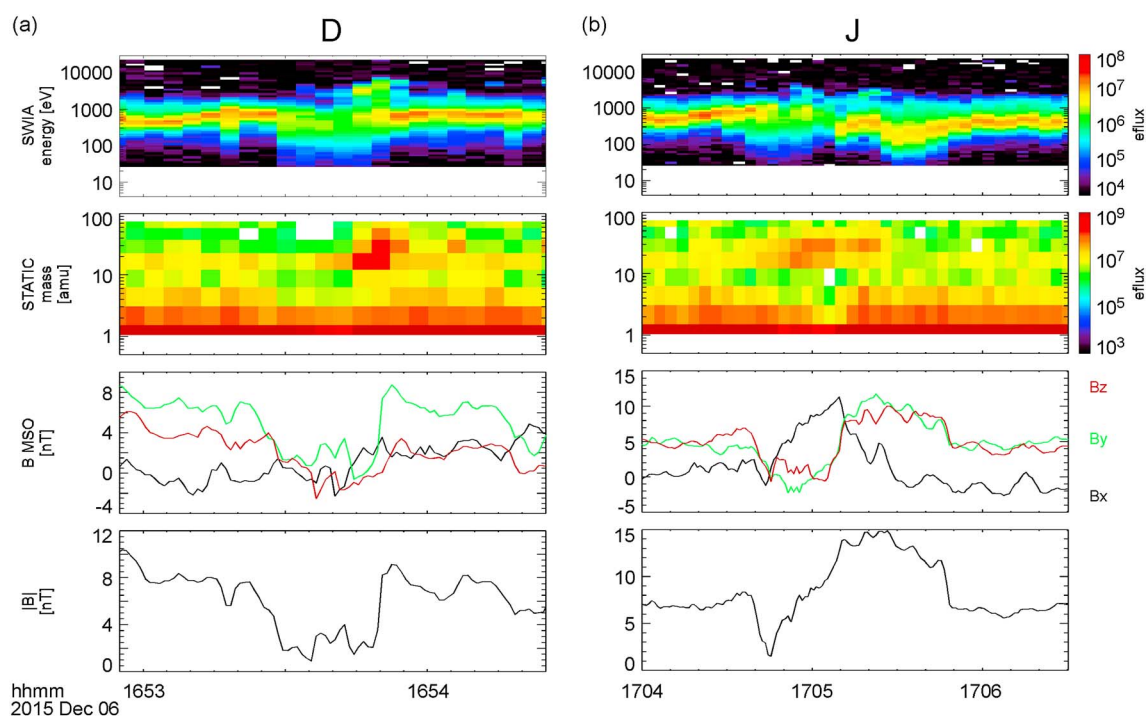


Figure 4. Two examples for the magnetic field signatures for the observed boundary oscillation events. (a and b) The magnetic field maxima do not coincide with the heavy ion encounters. This is a signature of KH instability and not a signature of flux transfer events.

Now we will determine whether these boundary oscillations can be a consequence of another phenomenon. We consider two such phenomena: Flux transfer events and upstream pressure perturbations. We observe that the magnetic field maxima do not coincide with the center of the regions of heavy ion encounters (see Figure 4). This signature has been reported for KH vortices at Earth where the magnetic field maxima coincide with the edges of the vortices, not at their center [Kavosi and Raeder, 2015]. This occurs because the magnetic pressure in combination with the thermal pressure acts to balance the centrifugal force of the vortex motion. For a flux transfer event, the magnetic field maximum occurs at its center [Kavosi and Raeder, 2015]. Thus, our observations are inconsistent with flux transfer events.

Upstream pressure perturbations are known to cause magnetopause oscillations at Earth [Song *et al.*, 1988]. There are two modes of oscillations that can be triggered by these upstream pressure perturbations: (1) Surface waves on the magnetopause caused by brief transient variations of the solar wind pressure and (2) long-period variation of the magnetopause caused by long-period variations in the solar wind pressure. The time period that distinguishes these two kinds of variation is $T = L_b/V_S$ where L_b is the distance along the boundary from the subsolar point to the terminator and V_S is the sheath velocity. For Earth this is about 20 min [Song *et al.*, 1988]. So essentially this corresponds to the longest period of the eigenmode for the Earth's magnetopause. Magnetopause oscillations that are caused by upstream pressure variations with periodicities longer than 20 min should damp out quickly. If we assume a similar scenario for the sheath-ionospheric boundary at Mars, we obtain $T = 4238\pi/(2 \times 241) = 28$ s for the surface waves. Here we use a distance of 4238 km as the distance from the center of the planet to the subsolar point. Our observed waves have a much longer period of 3 min, and if they are indeed caused by upstream pressure perturbations with a periodicity of 3 min, the boundary oscillations should damp out quickly and we should only observe few oscillation events. Upstream pressure perturbation is an unlikely candidate for the observed boundary oscillations since we observe more than 10 boundary oscillation events as depicted in Figure 1.

4. Summary

Here we reported ionospheric-sheath boundary oscillations at Mars observed by MAVEN as it ventured from the ionosphere to the sheath. The aim of our investigation was to determine whether these boundary oscillations were caused by KH instability. Using centrifugal force arguments, we first predicted the signatures of

fully rolled up KH vortices at Mars. Comparing these predictions with our observations, we concluded that the observed boundary oscillations are KH vortices that are in their development phase. We also excluded our observed phenomenon from flux transfer events and boundary oscillations induced by upstream pressure perturbations.

The following signatures enabled us to decipher the observed boundary oscillations as KH vortices in their development phase:

1. A fraction of sheath ions, H^+ , move faster than the mean sheath velocity. This is one of our predictions for the KH vortices and should be observed for sheath ions adjacent to the upper part of the vortex. This signature also enabled us to distinguish KH vortices from mass loading phenomena in which the ionospheric ions should slow down and not accelerate.
2. Heavy ions (O^+ and O_2^+) move antisunward faster than the mean ionospheric velocity. According to our predictions this is expected in the upper part of the vortex, and the observed heavy ion velocities are much higher than what would be expected from mass loading at the mass loading boundary.
3. A fraction of sheath ions, H^+ , have significantly slowed down compared to the mean sheath flow velocity. According to our predictions, a fully rolled up vortex should have sheath ions that move sunward. The absence of sunward moving ions but the presence of slowed down sheath ions are indicative of vortices that are not fully rolled up.
4. The magnetic field maxima do not coincide with the center of boundary oscillation events. This is a characteristic of KH vortices and not a characteristic of flux transfer events.
5. We observe more than 10 boundary oscillation events with a periodicity of 3 min. Such long-duration boundary oscillations, if caused by pressure perturbations, should damp out quickly, and we should not observe many boundary oscillation events.

We interpret that these non-fully developed vortices are consequences of the low growth rate of the KH instability and the small system size of Mars. These KH vortices may develop into fully rolled up states farther downstream.

Acknowledgments

This work was supported by NASA and was partially supported by the CNES. G. A. DiBraccio was supported by a NASA Postdoctoral Program appointment at the NASA Goddard Space Flight Center, administered by Universities Space Research Association through a contract with NASA. We thank Paul Song for useful discussions. MAVEN data are publicly available through the Planetary Data System.

References

- Acuña, M. H., et al. (1998), Magnetic field and plasma observations at Mars: Initial results of the Mars Global Surveyor mission, *Science*, 279, 1676–1680.
- Amerstorfer, U. V., N. V. Erkaev, D. Langmayr, and H. K. Biernat (2007), On Kelvin-Helmholtz instability due to the solar wind interaction with unmagnetized planets, *Planet. Space Sci.*, 55, 1811–1816.
- Boardsen, S. A., T. Sundberg, J. A. Slavin, B. J. Anderson, H. Korth, S. C. Solomon, and L. G. Blomberg (2010), Observations of Kelvin-Helmholtz waves along the dusk-side boundary of Mercury's magnetosphere during MESSENGER's third flyby, *Geophys. Res. Lett.*, 37, L12101, doi:10.1029/2010GL043606.
- Brace, L. H., R. F. Theis, and W. R. Hoegy (1982), Plasma clouds above the ionopause of Venus and their implications, *Planet. Space Sci.*, 30, 29–37.
- Brain, D. A., A. H. Baker, J. Briggs, J. P. Eastwood, J. S. Halekas, and T.-D. Phan (2010), Episodic detachment of Martian crustal magnetic fields leading to bulk atmospheric plasma escape, *Geophys. Res. Lett.*, 37, L14108, doi:10.1029/2010GL043916.
- Chandrasekhar, S. (1961), *Hydrodynamic and Hydromagnetic Stability*, Oxford Univ. Press, New York.
- Cahill, L. J., Jr., and J. R. Winckler (1992), Periodic magnetopause oscillations observed with the GOES satellites on March 24, 1991, *J. Geophys. Res.*, 97(A6), 8239–8243, doi:10.1029/92JA00433.
- Chaston, C. C., M. Wilber, F. S. Mozer, M. Fujimoto, M. L. Goldstein, M. Acuña, H. Rème, and A. Fazakerley (2007), Mode conversion and anomalous transport in Kelvin-Helmholtz vortices and kinetic Alfvén waves at the Earth's magnetopause, *Phys. Rev. Lett.*, 99(17), 175004.
- Chen, Q., A. Otto, and L. C. Lee (1997), Tearing instability, Kelvin-Helmholtz instability, and magnetic reconnection, *J. Geophys. Res.*, 102(A1), 151–161, doi:10.1029/96JA03144.
- Connerney, J. E. P., J. Espley, P. Lawton, S. Murphy, J. Odum, R. Oliverson, and D. Sheppard (2015), The MAVEN magnetic field investigation, *Space Sci. Rev.*, 195, 257–291, doi:10.1007/s11214-015-0169-4.
- Delamere, P. A., R. J. Wilson, S. Eriksson, and F. Bagenal (2013), Magnetic signatures of Kelvin-Helmholtz vortices on Saturn's magnetopause: Global survey, *J. Geophys. Res. Space Physics*, 118, 393–404, doi:10.1029/2012JA018197.
- Duru, F., D. A. Gurnett, D. D. Morgan, R. Lundin, I. H. Duru, J. D. Wittingham, and R. A. Frahm (2014), Dayside episodic ion outflow from Martian magnetic cusps and/or magnetosheath boundary motion associated with plasma oscillations, *Geophys. Res. Lett.*, 41, 3344–3350, doi:10.1002/2014GL059954.
- Ershkovich, A. I. (1980), Kelvin-Helmholtz instability in type-1 comet tails and associated phenomena, *Space Sci. Rev.*, 25, 3–34.
- Espley, J. R., P. A. Cloutier, D. A. Brain, D. H. Crider, and M. H. Acuña (2004), Observations of low-frequency magnetic oscillations in the Martian magnetosheath, magnetic pileup region, and tail, *J. Geophys. Res.*, 109, A07213, doi:10.1029/2003JA010193.
- Eastwood, J. P., D. A. Brain, J. S. Halekas, J. F. Drake, T. D. Phan, M. Øieroset, D. L. Mitchell, R. P. Lin, and M. Acuña (2008), Evidence for collisionless magnetic reconnection at Mars, *Geophys. Res. Lett.*, 35, L02106, doi:10.1029/2007GL032289.
- Fairfield, D. H., A. Otto, T. Mukai, S. Kokubun, R. P. Lepping, J. T. Steinberg, A. J. Lazarus, and T. Yamamoto (2000), Geotail observations of the Kelvin-Helmholtz instability at the equatorial magnetotail boundary for parallel northward fields, *J. Geophys. Res.*, 105(A9), 21,159–21,173, doi:10.1029/1999JA000316.
- Fairfield, D. H., C. J. Farrugia, T. Mukai, T. Nagai, and A. Federov (2003), Motion of the dusk flank boundary layer caused by solar wind pressure changes and the Kelvin-Helmholtz instability: 10–11 January 1997, *J. Geophys. Res.*, 108(A12), 1460, doi:10.1029/2003JA010134.

- Fujimoto, M., T. Tonooka, and T. Mukai (2003), Vortex-like fluctuations in the magnetotail flanks and their possible roles in plasma transport, in *Earth's Low-Latitude Boundary Layer*, edited by P. T. Newell and T. Onsager, pp. 241–251, AGU, Washington, D. C., doi:10.1029/133GM24.
- Gershman, D. J., J. M. Raines, J. A. Slavin, T. H. Zurbuchen, T. Sundberg, S. A. Boardsen, B. J. Anderson, H. Korth, and S. C. Solomon (2015), MESSENGER observations of multiscale Kelvin-Helmholtz vortices at Mercury, *J. Geophys. Res. Space Physics*, *120*, 4354–4368, doi:10.1002/2014JA020903.
- Gurnett, D. A., D. D. Morgan, F. Duru, F. Akalin, J. D. Winningham, R. A. Frahm, E. Dubinin, and S. Barabash (2010), Large density fluctuations in the Martian ionosphere as observed by the Mars Express radar sounder, *Icarus*, *206*, 83–94.
- Gunell, H., et al. (2008), Shear driven waves in the induced magnetosphere of Mars, *Plasma Phys. Controlled Fusion*, *50*, 074018.
- Halekas, J. S., J. P. Eastwood, D. A. Brain, T. D. Phan, M. Øieroset, and R. P. Lin (2009), In situ observations of reconnection Hall magnetic fields at Mars: Evidence for ion diffusion region encounters, *J. Geophys. Res.*, *114*, A11204, doi:10.1029/2009JA014544.
- Halekas, J. S., D. A. Brain, and J. P. Eastwood (2011), Large-amplitude compressive “sawtooth” magnetic field oscillations in the Martian magnetosphere, *J. Geophys. Res.*, *116*, A07222, doi:10.1029/2011JA016590.
- Halekas, J. S., E. R. Taylor, G. Dalton, G. Johnson, D. W. Curtis, J. P. McFadden, D. L. Mitchell, R. P. Lin, and B. M. Jakosky (2013), The solar wind ion analyzer for MAVEN, *Space Sci. Rev.*, *195*, 125–151, doi:10.1007/s11214-013-0029-z.
- Halekas, J. S., et al. (2015), Time-dispersed ion signatures observed in the Martian magnetosphere by MAVEN, *Geophys. Res. Lett.*, *42*, 8910–8916, doi:10.1002/2015GL064781.
- Halekas, J. S., et al. (2016), Plasma clouds and snowplows: Bulk plasma escape from Mars observed by MAVEN, *Geophys. Res. Lett.*, *43*, 1426–1434, doi:10.1002/2016GL067752.
- Hara, T., et al. (2015), Estimation of the spatial structure of a detached magnetic flux rope at Mars based on simultaneous MAVEN plasma and magnetic field observations, *Geophys. Res. Lett.*, *42*, 8933–8941, doi:10.1002/2015GL065720.
- Harada, Y., et al. (2015), Magnetic reconnection in the near-Mars magnetotail: MAVEN observations, *Geophys. Res. Lett.*, *42*, 8838–8845, doi:10.1002/2015GL065004.
- Harada, Y., et al. (2016), MAVEN observations of energy-time dispersed electron signatures in Martian crustal magnetic fields, *Geophys. Res. Lett.*, *43*, 939–944, doi:10.1002/2015GL067040.
- Hasegawa, H. (2012), Structure and dynamics of the magnetopause and its boundary layers, *Monogr. Environ. Earth Planets*, *1*(2), 71–119, doi:10.5047/meep.2012.00102.0071.
- Hasegawa, H., M. Fujimoto, T.-D. Phan, H. Réme, A. Balogh, M. W. Dunlop, C. Hashimoto, and R. TanDokoro (2004), Transport of solar wind into Earth's magnetosphere through rolled-up Kelvin-Helmholtz vortices, *Nature*, *430*, 755–758.
- Hasegawa, H., M. Fujimoto, K. Takagi, Y. Saito, T. Mukai, and H. Réme (2006), Single-spacecraft detection of rolled-up Kelvin-Helmholtz vortices at the flank magnetopause, *J. Geophys. Res.*, *111*, A09203, doi:10.1029/2006JA011728.
- Hasegawa, H., et al. (2009), Kelvin-Helmholtz waves at the Earth's magnetopause: Multiscale development and associated reconnection, *J. Geophys. Res.*, *114*, A12207, doi:10.1029/2009JA014042.
- Johnson, J. R., S. Wing, and P. A. Delamere (2014), Kelvin-Helmholtz instability in planetary magnetospheres, *Space Sci. Rev.*, *184*, 1–31.
- Kavosi, S., and J. Raeder (2015), Ubiquity of Kelvin-Helmholtz waves at Earth's magnetopause, *Nat. Commun.*, *6*, 7019.
- Kivelson, M. G., and S.-H. Chen (1995), The magnetopause: Surface waves and instabilities and their possible dynamical consequences, in *Physics of the Magnetopause*, edited by P. Song, B. U. Ö. Sonnerup, and M. F. Thomsen, AGU, Washington, D. C., doi:10.1029/GM090p0257.
- Liljeblad, E., T. Sundberg, T. Karlsson, and A. Kullen (2015), Statistical investigation of Kelvin-Helmholtz waves at the magnetopause of Mercury, *J. Geophys. Res. Space Physics*, *119*, 9670–9683, doi:10.1002/2014JA020614.
- Lundin, R., A. Zakharov, R. Pellinen, S. W. Barabash, H. Borg, E. M. Dubinin, B. Hultqvist, H. Koskinen, I. Liede, and N. Pissarenko (1990), ASPERA/Phobos measurements of the ion outflow from the Martian ionosphere, *Geophys. Res. Lett.*, *17*, 873–876.
- Lundin, R., E. M. Dubinin, H. Koskinen, O. Norberg, N. Pissarenko, and S. W. Barabash (1991), On the momentum transfer of the solar wind to the Martian topside ionosphere, *Geophys. Res. Lett.*, *18*, 1059–1062.
- Masters, A., et al. (2010), Cassini observations of a Kelvin-Helmholtz vortex in Saturn's outer magnetosphere, *J. Geophys. Res.*, *115*, A07225, doi:10.1029/2010JA015351.
- Masters, A., N. Achilleos, J. C. Cutler, A. J. Coates, M. K. Dougherty, and G. H. Jones (2012), Surface waves on Saturn's magnetopause, *Planet. Space Sci.*, *65*, 109–121.
- McFadden, J. P., et al. (2015), The MAVEN Suprathermal and Thermal Ion Composition (STATIC) instrument, *Space Sci. Rev.*, *195*, 199–256.
- Miura, A. (1992), Kelvin-Helmholtz instability at the magnetospheric boundary: Dependence on the magnetosheath sonic Mach number, *J. Geophys. Res.*, *97*(A7), 10,655–10,675, doi:10.1029/92JA00791.
- Miura, A. (1995), Kelvin-Helmholtz instability at the magnetopause: Computer simulations, in *Physics of the Magnetopause*, *Geophys. Monogr. Ser.*, vol. 90, edited by P. Song, B. U. Ö. Sonnerup, and M. F. Thomsen, pp. 285–291, AGU, Washington, D. C.
- Miura, A., and P. L. Pritchett (1982), Nonlocal stability analysis of the MHD Kelvin-Helmholtz instability in a compressible plasma, *J. Geophys. Res.*, *87*(A9), 7431–7444, doi:10.1029/JA087iA09p07431.
- Morgan, D. D., D. A. Gurnett, F. Akalin, D. A. Brain, J. S. Leisner, F. Duru, R. A. Frahm, and J. D. Winningham (2011), Dual-spacecraft observation of large-scale magnetic flux ropes in the Martian ionosphere, *J. Geophys. Res.*, *116*, A02319, doi:10.1029/2010JA016134.
- Möstl, U. V., N. V. Erkaev, M. Zellinger, H. Lammer, H. Gröller, H. K. Biernat, and D. Korovin (2011), The Kelvin-Helmholtz instability at Venus: What is the unstable boundary?, *Icarus*, *216*, 476–484.
- Nykyri, K., and A. Otto (2001), Plasma transport at the magnetospheric boundary due to reconnection in Kelvin-Helmholtz vortices, *Geophys. Res. Lett.*, *28*, 3565–3568, doi:10.1029/2001GL013239.
- Nykyri, K., A. Otto, B. Lavraud, C. Mouikis, L. M. Kistler, A. Balogh, and H. Réme (2006), Cluster observations of reconnection due to the Kelvin-Helmholtz instability at the dawnside magnetospheric flank, *Ann. Geophys.*, *24*, 2619–2643.
- Ogilvie, K. W., and R. J. Fitzenreiter (1989), The Kelvin-Helmholtz instability at the magnetopause and inner boundary layer surface, *J. Geophys. Res.*, *94*(A11), 15,113–15,123, doi:10.1029/JA094iA11p15113.
- Penz, T., et al. (2004), Ion loss on Mars caused by the Kelvin-Helmholtz instability, *Planet. Space Sci.*, *52*, 1157–1167.
- Palermo, F., M. Faganello, F. Califano, F. Pegoraro, and O. Le Contel (2012), The role of the magnetosonic Mach number on the evolution of Kelvin-Helmholtz vortices, *EAS Publ. Ser.*, *58*, 91–94.
- Pope, S. A., M. A. Balikhin, T. L. Zhang, A. O. Fedorov, M. Gedalin, and S. Barabash (2009), Giant vortices lead to ion escape from Venus and re-distribution of plasma in the ionosphere, *Geophys. Res. Lett.*, *36*, L07202, doi:10.1029/2008GL036977.
- Rubin, M., K. C. Hansen, M. R. Combi, L. K. S. Daldorff, T. I. Gombosi, and V. M. Tenishev (2012), Kelvin-Helmholtz instabilities at the magnetic cavity boundary of comet 67P/Churyumov-Gerasimenko, *J. Geophys. Res.*, *117*, A06227, doi:10.1029/2011JA017300.

- Ruhunusiri, S., J. S. Halekas, J. E. P. Connerney, J. R. Espley, J. P. McFadden, D. E. Larson, D. L. Mitchell, C. Mazelle, and B. M. Jakosky (2015), Low-frequency waves in the Martian magnetosphere and their response to upstream solar wind driving conditions, *Geophys. Res. Lett.*, *42*, 8917–8924, doi:10.1002/2015GL064968.
- Seon, J., L. A. Frank, A. J. Lazarus, and R. P. Lepping (1995), Surface waves on the tailward flanks of the Earth's magnetopause, *J. Geophys. Res.*, *100*(A7), 11,907–11,922, doi:10.1029/94JA03314.
- Song, P., R. C. Elphic, and C. T. Russell (1988), ISEE 1 and 2 observation of the oscillating magnetopause, *Geophys. Res. Lett.*, *15*, 744–747.
- Sundberg, T., S. A. Boardsen, J. A. Slavin, L. G. Blomberg, J. A. Cumnock, S. C. Solomon, B. J. Anderson, and H. Korth (2011), Reconstruction of propagating Kelvin-Helmholtz vortices at Mercury's magnetopause, *Planet. Space Sci.*, *59*, 2051–2057.
- Takagi, K., C. Hashimoto, H. Hasegawa, M. Fujimoto, and R. TanDokoro (2006), Kelvin-Helmholtz instability in a magnetotail flank-like geometry: Three-dimensional MHD simulations, *J. Geophys. Res.*, *111*, A08202, doi:10.1029/2006JA011631.
- Terada, N., S. Machida, and H. Shinagawa (2002), Global hybrid simulation of the Kelvin-Helmholtz instability at the Venus ionopause, *J. Geophys. Res.*, *107*(A12), 1471, doi:10.1029/2001JA009224.
- Taylor, M. G. G. T., et al. (2012), Spatial distribution of rolled up Kelvin-Helmholtz vortices at Earth's dayside and flank magnetopause, *Ann. Geophys.*, *30*, 1025–1035.
- Vignes, D., M. H. Acuña, J. E. P. Connerney, D. H. Crider, H. Rème, and C. Mazelle (2004), Magnetic flux ropes in the Martian atmosphere: Global characteristics, *Space Sci. Rev.*, *111*, 223–231.
- Winningham, J. D., et al. (2006), Electron oscillations in the induced Martian magnetosphere, *Icarus*, *182*, 360–370.
- Wolff, R. S., B. E. Goldstein, and C. M. Yeates (1980), The onset and development of Kelvin-Helmholtz instability at the Venus ionopause, *J. Geophys. Res.*, *85*(A13), 7697–7707, doi:10.1029/JA085iA13p07697.